Failure Modes and Effects Analysis (FMEA) of GNSS Aviation Applications

Carl D. Milner and Prof. Washington Y. Ochieng
Centre for Transport Studies
Department of Civil and Environmental Engineering
Imperial College London
South Kensington Campus
London SW7 2AZ
carl.milner05@imperial.ac.uk
+44 (0)20 7594 6024

Abstract

Integrity risk is the product of the probabilities of the occurrence of a failure and that it is not detected the integrity monitoring algorithm. For stand-alone GPS applications, the challenge remains to provide a 'realistic as is reasonable' model of failure occurrence both for the design of integrity monitoring algorithms and also the derivation of performance requirements for operations which require their use. Furthermore, the baseline on-board integrity prediction function includes a conservative bound which limits the availability of system. In order to meet these challenges, a Failure Modes and Effects Analysis (FMEA) is required which characterises the form of failures and their impact on the system.

The application of the GPS SPS failure model does not always represent the characteristics of the various possible failures and their characteristics. The GPS SPS defines the probability of failure through a binary function whose range error magnitude parameter determines whether the system is operating nominally or under the presence of a failure. However, many applications assume worst case bias values at the same probability which may be overtly conservative. It is the goal of this paper to pave the way for a new concept in failure definition which provides greater detail of the probabilities of failures over a range of biases. It is shown that even under conservative assumptions; this model leads to comparable values to those provided within the GPS specification but does not excessively account for the likeliness of failure at higher bias values.

Furthermore, the determination of missed detection probabilities of the monitoring function may also incorporate conservative modelling assumptions. Initial results are presented for an accelerated integration of the integrity risk for weighted RAIM. This approach uses a number of numerical approximations whose errors are fully accounted and therefore avoids unnecessary conservative assumptions to guarantee integrity performance. Results for APVI operations using the new protection level computation find a marked 30% increase in availability over conventional weighted RAIM.

Introduction

Currently, the GPS standard positioning service (SPS) is designed to meet a minimum performance standard for civilian use specified in (GPS SPS, 2001)[1]. The specification allows for major service failures in very rare cases - three per year over the entire constellation. A major service failure is defined by a range error exceeding either 30m or 4.42 times the user range accuracy at one sigma (4.42σ). This definition is used within the aviation industry and other safety critical applications in order to quantify the probability of a satellite failure. Due to the GPS SPS not having provision for an integrity service it is necessary this function must be added such that safety critical applications such as aviation are able to meet their requirements. A number of aviation operations require integrity risk

[1] Note that at the time of paper submission a new version of the GPS SPS was released (DoD GPS SPS, 2008). This alters slightly the probability of failure occurrence and removes the 30m boundary, using just the 4.42×URA in the definition. However, the premise for the development of a new failure characterisation concept remains unchanged.

be bounded by 10^{-7} per hour. Under the GPS SPS specifications, the probability of failure equates to approximately 10^{-4} per hour (Lee *et al*, 1996) and therefore the integrity monitoring function must detect failures at the level of $1\text{-}10^{-3}$ ($10^{-7} = 10^{-4} \times 10^{-3}$) in order to meet the requirements.

This paper considers stand-alone GPS with the additional functionality of receiver autonomous integrity monitoring (RAIM). In developing RAIM algorithms it is commonly assumed that a failure occurs with a probability of 10^{-4} per hour and that there is no prior knowledge to the magnitude of a possible failure. This leads to the requirement on RAIM of a probability of missed detection of 10^{-3} for all biases (Lee *et al*, 1996). This paper proposes to challenge this assumption and allow advanced RAIM algorithms to be developed using a more sophisticated failure model.

Stand-alone GPS operations are currently being used for en-route and in some states NPA operations. However, more stringent operations such as APVI are unable to meet reasonable availability levels using the baseline weighted least squares RAIM algorithm (RTCA DO-229D, 2006). This is in part due to the use of a conservative buffer on the protection level (Brown & Chin, 1997). A numerical method is presented in this paper, conceived as a reasonable compromise between an overly conservative approximation bound and a full Monte Carlos simulation. By accounting for numerical errors and tuning for accuracy and speed, a practical numerical method is derived in the second half of the paper which can improve APVI availability whilst protecting against excessive computational inefficiency.

Failure Modes Database

The Failure Modes and Effects Analysis (FMEA) project run by Imperial College London began by enhancing the capture and characterisation of GPS failure modes. This has been achieved through monitoring and analysis of GPS signals and a comprehensive literature review, incorporating most importantly RTCA Paper 034-01/SC159-867 (RTCA 034-01, 1998) released from the GPS service providers. In some cases, the data analysed in the monitoring program (UK CAA, 2007) required consolidating with the aberration description given in (RTCA 034-01, 1998). The standard approach was to use the probability and other parameters provided by (RTCA 034-01, 1998) but to augment the magnitude and type of failure observed.

Table 1 shows an overview of the failure modes database. Only the failure modes which present an integrity threat are included, those which are guaranteed to be detected on-board the satellite or almost instantly by the user are excluded simply as continuity risks (e.g. clock phase run-off due to oscillator or oven failure 54000km/hr). An excellent review of the types of failure mode is given in (Bhatti & Ochieng, 2007)

Failure Mode	Probability of Occurrence	Type	Magnitude
Clock Jump	1.0e-1 / SV / year	STEP	0-30m
Clock Frequency Jump/Drift	1.0e-1 /SV / year	RAMP	2.5m / s
Clock Drift/Phase-Runoff (Atomic Clock Power Supply)	6.6e-3 / SV / year	RAMP	54km / hr
Clock Drift/Phase-Runoff (Atomic Clock Electronics)	1.1e-2 / SV / year	RAMP	10m / hr
Clock Drift/Phase-Runoff (Atomic Clock Servo Mechanism)	1.0e-2 / SV / year	RAMP	10m / hr
Clock Drift/Phase-Runoff (Atomic Clock Cs/Rb tube)	3.3e-1 / SV / year	RAMP	10m / hr
Clock Drift/Phase-Runoff (Atomic Clock Tuning Register)	2.1e-5 / SV / year	RAMP	2164m / hr
Clock Drift/Phase-Wander (Atomic Clock)	1.0 / SV / year	WANDER	1.0m / hr
Clock Frequency Jump	1.0 / SV / year	RAMP	2.0m / hr
FSDU Upsets	3.0e-1 / SV / year	STEP	0-30m
Meteor Impact (Delta-V)	TBD	RAMP	0-10m / hr

MCS Upload Error (Bad Earth Orientation Data)	5.2e-8 / constellation / year	RAMP	0.0056m / s
MCS Upload Error (Single Freq. Ion. Model)	2.4e-2 / upload	NOISE	13.7m (1σ)
Operational Error (Too early SV return to 'healthy' status)	5.0e-8 / constellation / year	STEP : RAMP	120m : 5m / hr
Operational Error (Not flagged 'unhealthy')	5.0e-5 / constellation / year	RAMP	120m / hr
Operational Error (Incorrect database control element)	6.2e-9 / constellation / year	RAMP	0.0-0.3m / sec
Orbit Mis-modelling	Empirically Derived	VARIES	Empirically Derived

Table 1: Failure Modes Database Summary

Bias Error Model

The current failure definition for a GPS satellite is as follows:

$$\mathbf{P(B > T) = p_{failure}} \tag{1}$$
$$\mathbf{P(B < T) = 1 - p_{failure}} \tag{2}$$

where $\mathbf{p_{failure}}$ is derived from the three major service failures per year (Lee *et al*, 1996), **B** is the measurement bias and *T* is defined as above to be 30m or 4. 42σ.

The goal of the failure mode bias model is to generate a file which expresses the probability of the range error magnitude at a range of bias values (b_k's):

$$\mathbf{P(0 < B < b_1) = cdf_1} \tag{3}$$
$$\ldots\ldots\ldots\ \mathbf{P(b_i < B < b_{i+1}) = cdf_i} \tag{4}$$
$$\ldots\ldots\ldots\ \mathbf{P(b_{max-1} < B < b_{max}) = cdf_{max-1}} \tag{5}$$
$$\ldots\ldots\ldots\ \mathbf{P(b_{max} < B\ ) = cdf_{max}} \tag{6}$$

The **cdf** parameters are stored in the file to quantify the probability of a bias lying between the interval boundaries $\mathbf{\{b_k\}}$. It is clear from the above formulation that the choice of $\mathbf{b_i}$*'s* is an important factor. In order to demonstrate the concept the following values were used.

Bias values between 0 and 200m are taken at 1m intervals - 0:1:200.
Bias values between 200m and 1000m are taken at 10m intervals - 200:10:1000.
Bias values between 1000m and 2000m are taken at 100m intervals 1000:100:2000.
This results in a set of 292 **b** values.

This choice is somewhat arbitary at this stage, but without a demonstration of the required accuracy of the bias model within the design of a RAIM or other algorithm, a revision is not possible until a later phase in the research and exploration of the concept. However on the basis of the data processing undertaken within the FMEA project it was found that bias values beyond 2000m present an infitesimal threat to NPA operations. More stringent operations, under GPS and in the future Galileo will be sensitive to smaller biases still and as such the critical range 0-200m for which 1m was considered a reasonable resolution. If necessary it is feasible to reduce the separation between *b* values to improve accuracy at a later stage. The $\mathbf{b_{max}}$ of 2000m was chosen as a cut off for outliers as errors of this magnitude would be guaranteed to be detected to probabilities less than 10^{-15} by a suitable RAIM detection function. In any case $\mathbf{cdf_{max}}$ could be used to account for such events.

Given this framework it was necessary to convert the probability of each relevant failure mode record within the failure modes database to the format described above. In practical terms, the output of this process is a text file of two columns displaying the *b* values and associated **cdf**.

Observing the failure mode database summarised in Table 1, it is clear that two complications make the task of expressing each failure mode in the standard bias format described above. Firstly, the failure modes occur in a variety of ways and can be categorised as particular failure types (Bhatti & Ochieng, 2007). Secondly, the probabilities of occurrence are not specified in a standardised form.

With regard to the varying failure type it is noted that a step error may generate an instantaneous jump in the measurement bias from 0 metres to *B* metres whereas a ramp error grows at a particular rate. A number of assumptions are made implicit to the argument at this stage. Most importantly, ramp errors are assumed to possess a constant ramp error rate. If the true failure mode deviates greatly from this model, in a grossly exponential fashion for example, the failure mode type may be invalid, however of the failure modes characterised, such behaviour is not expected. An additional failure mode type would have to be defined if such a failure mode were discovered in light of GPS III or Galileo SV developments.

Due to the variation in time periods over which the failure mode probabilities are specified, the decision was taken to compute the instantaneous probability of a failure over a given bias range ($\mathbf{b_i}$ to $\mathbf{b_{i+1}}$). This is relevant to the user as it answers the question 'Given the GPS constellation at epoch $\mathbf{t_{now}}$ what are the probability of failures of each satellite at each bias?'. This diverges from the traditional approach of specifying probabilities over one hour or other time period. This is possible because of the failure mode exposure times are known in addition to assuming there is no temporal overlap of failure occurrences. If one assumes no overlapping of failures for a single SV then the probability of failure remains constant between neighbouring time points however close together. This is not true of measurement noise due to temporal and spatial correlation effects. Therefore, to determine the spacing of independent samples it is only the measurement noise decorrelation coefficient which must be considered. At each independent sample one can use the instantaneous bias failure model described above. Therefore, the task remains to describe a means to compute $\mathbf{P(\, b_i < B < b_{i+1} \mid t_{now}\,)}$ for each failure type.

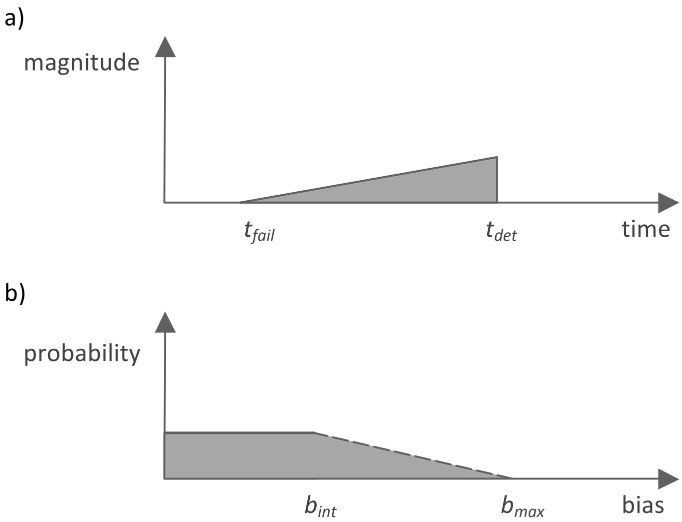

Figure 1: Ramp Error Type a) Magnitude vs. time b) Probability vs. bias (assumed model)

Ramp Error Type

A ramp error is one which the range measurement has a constant rate of growth from zero until the failure is detected and mitigated against as shown in Figure 1a. The basis for computing $\mathbf{P(\, b_i < B < b_{i+1} \mid t_{now}\,)}$ for the ramp error failure modes is to calculate the length of time the measurement error magnitude for a particular failure mode remains within the range $\mathbf{b_i < B < b_{i+1}}$. Given any time period (e.g. 1 hour) over which the probability of failure mode occurrence is stated in

Table 1, it is possible to determine the proportion of this time period which equates to the length of time the measurement error magnitude is within the relevant range.

e.g. Given a ramp error of 0.05m/s which occurs at 1e-5 per hour. This failure will take 20s to increase by 1m from 36m to 37m which is 5.556e-3 (20/3600) of one hour. Therefore:

$$\mathbf{P(\ 36m\ < B <\ 37m\ \mid\ t_{now}\ ) = \left(1e-5\right)\times\left(5.556e-3\ \right)= 5.556e-8} \tag{7}$$

However, consideration of the maximum exposure time is relevant for large bias magnitudes because the probability defined by (4) must incorporate the probability factor that the failure has not been detected and mitigated by the OCS. This has the effect of reducing the probability of larger biases being present due to a ramp error as shown in Figure 1b. The exposure time is specified as a range (denoted by $\mathbf{t_{low}}$ and $\mathbf{t_{high}}$) by the RTCA (e.g. 1.5 - 4.0 hours) (RTCA 034-01, 1998). Therefore we can deduce the following two relations:

$$\mathbf{P(\ detected\ \left| t_{now}\ -\ t_{fail}\ < dt_{low}\ \right)\ = 0.0} \tag{8}$$

$$\mathbf{P(\ detected\ \left| t_{now}\ -\ t_{fail}\ > dt_{high}\ \right)\ = 1.0} \tag{9}$$

From these two statements we can further deduce the maximum bias and a maximum undetectable (for this particular failure mode via the monitoring network) bias as shown in Figure 1b.

$$\mathbf{P(\ detected\ \left| B < b_{int}\ \right)\ = 0.0}\ \text{where}\ \mathbf{b_{int}\ = r\,dt_{low}} \tag{10}$$

$$\mathbf{P(\ detected\ \left| B > b_{max}\ \right)\ = 1.0}\ \text{where}\ \mathbf{b_{max}\ = r\,dt_{high}} \tag{11}$$

All that remains is to determine the probability of detection between these two bias magnitudes. Due to the lack of corroboration for the exposure time periods which relate to these two values, it is necessary to make an assumption with regard to the likelihood of detection and mitigation within the range. It is assumed that the probability of detection could be approximated by the form of a geometric series.

$$\mathbf{P(\ detected\ t_k\ ) = P\left(undetected\ t_{k-1}\ \right)\times P\left(detected\ t_k\ \middle| undetected\ t_{k-1}\ \right) = \left(1-q\right)^{k-1} q} \tag{12}$$

This makes intuitive sense because it results in low probabilities near the end of the range because the error would have to have remained undetected up to that point. The decorrelation of measurement noise which affects the detection of failures by the monitoring network could be interpreted as leading to a partially discrete system which gives the approximation extra validity. The graphs shown in Figure 2 demonstrate the form of the probability functions of detection and missed detection under this model.

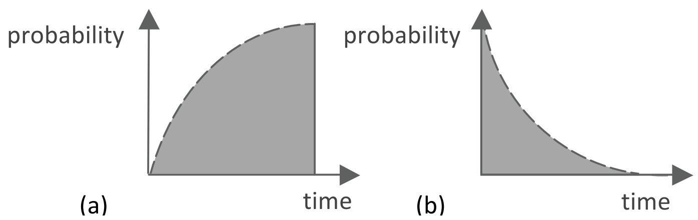

Figure 2: Probabilities of detection (a) and no detection (b) under the geometric

The aim of this model is not to accurately determine the probabilities but to provide the basis of a further approximation which would bound the probability densities shown in Figure 3. If the cumulative density function is defined to be linear over the range $\mathbf{b_{int}}$ to $\mathbf{b_{max}}$ then this would bound a density function similar in form to the geometric series, in fact any with a lessening negative gradient. The probability of the bias remaining undetected is then given by this linear cumulative density function.

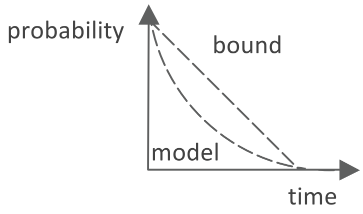

Figure 3: Bound of Geometric Series Model by linear function

Step Error Type

A step error differs from a ramp error in that its magnitude remains constant over time between the failure onset and mitigation following detection (Figure 4a). It is therefore simply necessary to integrate the probability density function with respect to time, which is equivalent to computing the area under the graph shown in Figure 4b, normalising to the time period specified in the failure mode probability of occurrence and then multiplying by the same probability.

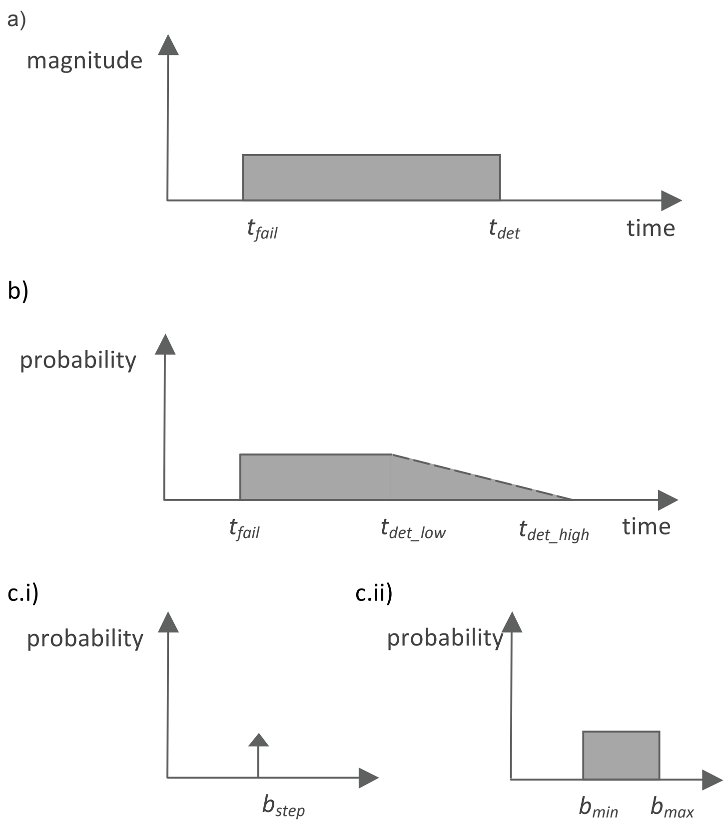

Figure 4: Step Error a) Failure mode magnitude vs. time b) Probability of failure present vs. time c.i) Single Value - probability vs. bias magnitude c.ii) Range of Values - probability vs. bias magnitude

In some cases the exact value of step error is not fully known and a range of values may be used to describe the failure's form. The two cases are shown in Figures 4c.i and 4c.ii.

Noise Error Type

Failure modes resulting in measurement noise are specified by a sigma value relating to an extra component of measurement noise. It is simply assumed the measurement noise is Gaussian in nature and a uninormal distribution is used to compute error magnitudes as shown in Figure 5.

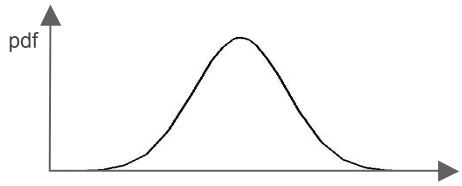

Figure 5: Noise Error Type Gaussian Model

Wander Error Type

The effect of a random wander error type is similar to a random noise component but the magnitude is a stochastic function of time. The random wander parameter, *k* represents a mean variation from a zero error magnitude over a particular time frame. The conservative assumption that detection only occurs at the end of the detection range specified in the failure mode database; contrary to the ramp error model type simplifies the analysis. The deviation from the mean is assumed to follow a Gaussian distribution whose mean variation grows at the rate specified by *k*.

Bias Model

It is possible to compute a total failure mode bias probability model which sums the probabilities for each failure mode within the standardised bias range. Also included is an empirically derived model for orbit modelling errors

$$\mathbf{P}\left(\mathbf{b}_i < \mathbf{B} < \mathbf{b}_{i+1}\right)_{total} = \sum_{\substack{failure\\modes}} \mathbf{P}\left(\mathbf{b}_i < \mathbf{B} < \mathbf{b}_{i+1}\right) \tag{13}$$

This summation is possible due to the assumption of failure mode independence.

In order to compare to the GPS standard, it is possible to compute the probability of a failure resulting in a bias magnitude of 30-2000m. The results of this summation with and without the addition of the orbit error model are given below:

$$\mathbf{P}\left(\mathbf{30} < \mathbf{B} < \mathbf{2000}\right)_{no\_orbit} = 8.916\text{e-}06 \tag{14}$$

$$\mathbf{P}\left(\mathbf{30} < \mathbf{B} < \mathbf{2000}\right)_{orbit} = 9.632\text{e-}06 \tag{15}$$

This compares with a value of *1.25e-5* per SV per hour (Lee *et al*, 1996).

Missed Alert Probabilities

In the previous section an overview of a novel characterisation of the GPS failure modes was given. The next step is to assess how these failures are currently dealt with by the RAIM algorithm. The ultimate goal is to combine the two phases seamlessly, yet firstly the improvement of missed alert probability estimation is achieved using a RAIM algorithm and the traditional failure model. The RAIM system model is summarised below, followed by a description of the accelerated numerical technique.

System Model

The foundation of the weighted least-squares RAIM formulation is the assumption of an overdetermined system of linear equations.

$$\mathbf{z} = \mathbf{Hx} + \boldsymbol{\varepsilon} \tag{16}$$

where:

- $\mathbf{z}$: n-dimensional vector of measurements
- $\mathbf{H}$: $\mathbf{n \times 4}$ - dimensional geometry matrix defined in the local horizontal frame, with the condition $\mathbf{n > 4}$
- $\mathbf{x}$: $\mathbf{4}$ - dimensional vector of unknowns (position and clock bias)
- $\boldsymbol{\varepsilon}$: $\mathbf{n}$ - dimensional vector of measurement errors

It is assumed that the measurement errors may be modelled as the sum of measurement noise **v** and measurement biases **b**:

$$\boldsymbol{\varepsilon} = \mathbf{b} + \mathbf{v} \tag{17}$$

and that the underlying measurement noise is normally distributed with covariance matrix $\boldsymbol{\Sigma}$ as follows:

$$\mathbf{v}' \sim \mathbf{N}(0, \boldsymbol{\Sigma}) \tag{18}$$

The linear equation (16) is assumed to have been normalised by down-weighting the measurements subject to their estimated measurement variances in (18). The resulting measurement errors **v** are then uncorrelated and of equal variance.

The weighted least squares estimate has been derived as follows (Walter and Enge, 1995):

$$\hat{\mathbf{x}}_{WLS} = \left(\mathbf{H}^T\mathbf{W}\mathbf{H}\right)^{-1}\mathbf{H}^T\mathbf{W}\mathbf{z} \tag{19}$$

where the down-weighting is defined by setting **W** to the inverse of $\boldsymbol{\Sigma}$, $\mathbf{W} = \boldsymbol{\Sigma}^{-1}$. The position error, the difference between the navigation position solution $\hat{\mathbf{x}}_{WLS}$ and the true position $\mathbf{x}_{true}$ may be defined from applying the WLS operator to the measurement error vector.

$$\mathbf{e} = \hat{\mathbf{x}}_{WLS} - \mathbf{x}_{true} = \left(\mathbf{H}^T\mathbf{W}\mathbf{H}\right)^{-1}\mathbf{H}^T\mathbf{W}\boldsymbol{\varepsilon} \tag{20}$$

The test statistic shall be defined as the magnitude of the parity vector $|\mathbf{p}|$, which is equivalent to the weighted least-squares residual defined in (Walter and Enge, 1995).

$$\mathbf{p} = \mathbf{P}\mathbf{z} = \mathbf{P}\boldsymbol{\varepsilon} \tag{21}$$

where P is the parity matrix as usually defined (Sturza, 1988).

A bias in the system is expressed simply by substituting a bias vector into equations 19 and 21.

$$\mathbf{ebias} = \left(\mathbf{H}^T\mathbf{W}\mathbf{H}\right)^{-1}\mathbf{H}^T\mathbf{W}\mathbf{b} \tag{22}$$

$$\mathbf{pbias} = \mathbf{P}\mathbf{b} \tag{23}$$

An important relation is the ratio of a measurement bias projected to both position and parity domains. This relation holds in the absence of measurement noise is defined by the slope parameter.

$$\mathbf{slope}_i = \frac{\mathbf{ebias}}{\mathbf{pbias}} = \frac{\left[\left(\mathbf{H}^T\mathbf{W}\mathbf{H}\right)^{-1}\mathbf{H}^T\mathbf{W}\right]_{i,3}}{\left[\mathbf{P}\right]_{i,3}} \tag{24}$$

However in the presence of noise, importantly the position error and parity vectors' stochastic components have known variances under the model, defined as follows:

$$\mathbf{Cov}(\mathbf{e}) = \left(\mathbf{H}^T\mathbf{W}\mathbf{H}\right)^{-1} \tag{25}$$

$$\mathbf{Cov}(\mathbf{p}) = \mathbf{P}\mathbf{P}^T = \mathbf{I}_{n-4} \tag{26}$$

In the ordinary least squares RAIM formulation, the stochastic components of **e** and **p** are independent. However, when down-weighting for unequal measurement variances, this relationship no longer applies and the cross-covariance between **e** and **p** is non-zero (Hwang & Brown, 2006)

$$\mathbf{Cov}(\mathbf{e},\mathbf{p}) = \mathbf{P}\mathbf{W}^T\mathbf{H}\left(\mathbf{H}^T\mathbf{W}\mathbf{H}\right)^{-1} \tag{27}$$

The effect of this non-zero cross correlation can be seen in the error-test statistic (ET) space shown in Figure 6.

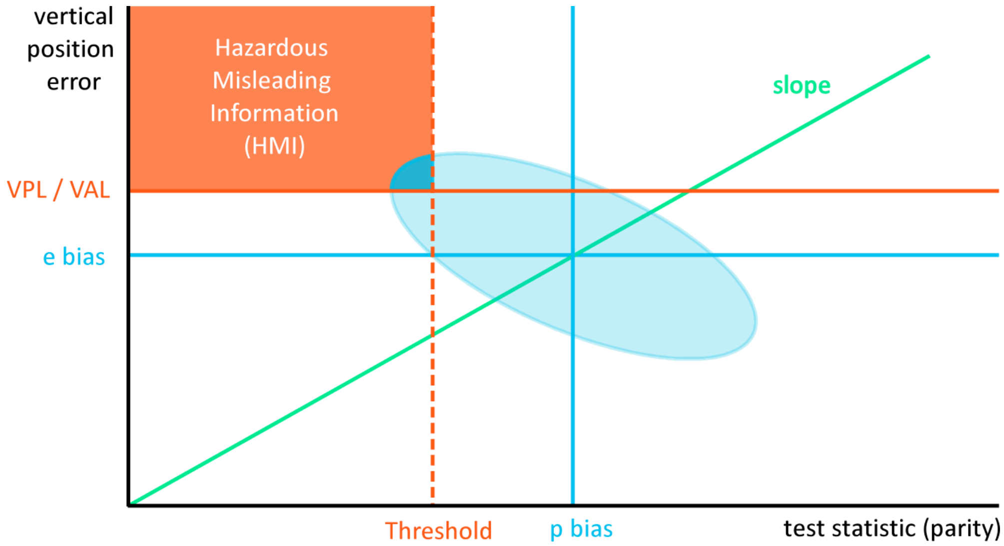

Figure 6: ET Diagram

The operational requirements for aviation are specified as functions of the probability of hazardous misleading information (HMI),alert limit and a false alarm rate. This false alarm rate may be used to derive the threshold for the parity test statistic used.

In order to derive vertical protection limit (VPL) the first step is the computation of a Minimal Detectable Bias (MDB_p) in the parity domain. The probability of missed detection (PMD), which is set by the RTCA at 0.001 by factoring the probability of a failed satellite 10^{-4} into the integrity risk requirement of 10^{-7}, is used as input to an inverse non-central chi-squared distribution function as follows:

$$\mathbf{MDB_p} = \sqrt{\lambda} \tag{28}$$

$$\lambda = \mathbf{Q}^{-1}\left(\mathbf{P_{MD}}, \mathbf{n-4}, \mathbf{T}\right) \tag{29}$$

such that

$$\mathbf{P_{MD}} = \mathbf{Q}\left(\mathbf{n-4}, \lambda, \mathbf{T}\right) = \int_0^T \chi^2_{pdf}\left(\mathbf{n-4}, \lambda, \mathbf{t}\right)\mathbf{dt} \tag{30}$$

This MDB_p shown in Figure 7 represents the smallest bias transformed into the parity domain which may remain undetected with a probability equal to the P_{MD}. Therefore larger biases are guaranteed not to lead to PHMI greater than the requirement. The calculation of VPL then projects this bias into the position domain by use of the slope parameter, as clearly demonstrated in Figure 7.

$$\mathbf{ebias_{MDB} = slope_i \times MDB_b} \tag{31}$$

However, this position error value is not guaranteed to provide a protective limit on the PHMI because biases less than the MDB_p may result in more of the probability density lying in the critical HMI region. Therefore an additional term is required (Angus, 2006) which protects against the variation in position error. This is simply the one-sided confidence interval of the position error at the significance of P_{MD}.

$$\mathbf{k\text{-}term = k_{MD} \times Cov(e)_{3,3}} \tag{32}$$

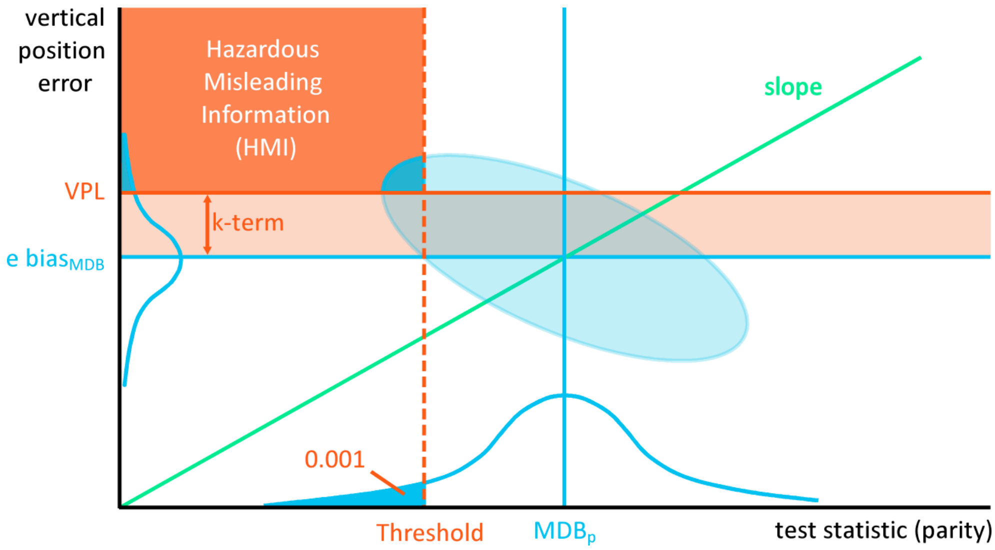

Figure 7: ET diagram - Derivation of VPL

This process is the baseline computation, for predicting RAIM availability specifically for vertical guided operations in this case. Although the process is similar for the 2D horizontal case, the vertical requirements are known to be the most critical. There are two points at which this process excessively over-bounds the true PHMI and leads to an exaggerated VPL prediction. Firstly the use of a fixed bias is chosen to account for the bias magnitude ambiguity and is computed on the basis of detectability alone, whereas the definition of integrity risk includes the joint probability of a positioning failure (the VPL or VAL is exceeded by the position error) and no detection. Secondly, the k-term is applied at this MDB_p whereas it is designed to account for position variation at lower biases and its relevance increases as the bias decreases.

The following sections describe how by using the bias failure model described above and integrating an approximation of the joint position error and parity distribution, these two problems may be avoided. A Gaussian approximation of the joint distribution is now considered.

Gaussian Approximation

The cross-correlation between the parity and error vectors must be considered when determining a method which computes the PHMI without conservatively de-coupling the worst case marginal distributions.

A Gaussian approximation is used to model the joint distribution between the vertical position error and the magnitude of the parity vector. This bi-variate Gaussian has a mean defined by the ebias value and the magnitude of pbias, $(\mathbf{ebias, pbias})$. The covariance matrix is formed from the covariance matrices of the position error, parity vector and the cross-covariance matrix.

$$\mathbf{\Sigma}_{pe} = \begin{bmatrix} \mathbf{c}_{pp} & \mathbf{c}_{pe} \\ \mathbf{c}_{ep} & \mathbf{c}_{ee} \end{bmatrix} \tag{33}$$

where

$$\mathbf{c}_{pp} = \mathbf{I}_{n-4} \tag{34}$$

$$\mathbf{c}_{ee} = \left(\mathbf{H}^T\mathbf{W}\mathbf{H}\right)^{-1} \tag{35}$$

$$\mathbf{c}_{pe} = \left\| \left[\mathbf{P}\mathbf{W}^T\mathbf{H}\left(\mathbf{H}^T\mathbf{W}\mathbf{H}\right)^{-1} \right]_3 \right\|_i \tag{36}$$

The modulus operation applied to the vertical column of the $\mathbf{Cov}(\mathbf{e},\mathbf{p})$ matrix is required to ensure the worst case coupling in variation between the parity test statistic and vertical position error. A conservative approximation is therefore preferred to a more accurate but less reliable approximation.

Integration Technique

The WRAIM integration process searches for a worst case bias over the hazardous region. The probability distribution of position failure is a monotonically increasing function and the probability distribution of no detection is a monotonically decreasing function. Therefore the probability of a missed detection occurring as a function of bias has a single maximum over this range. This ensures that performing a nested search converges to an optimal solution and is quicker, more elegant solution than finding the worst case bias simply by an incremental search.

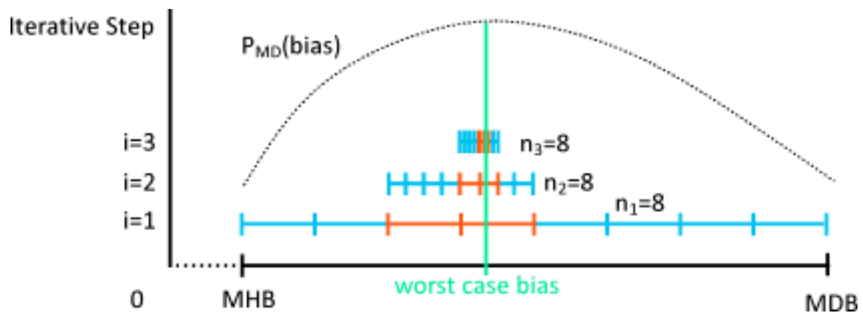

Figure 8: Iterative Worst Case Bias Search

Figure 8 shows an example of the nested worst case bias search. Here the order of the search is eight, which requires the evaluation of nine integrals. At each iterative step the worst case is selected and in addition it's two neighbours which form the boundary of the following step.

The numerical integration at each bias must take account of the correlation between parity vector and position error. This is achieved by computing the marginal position error distribution conditional on the magnitude of parity vector under the Gaussian bivariate assumption described above in equation 33. The conditional distribution of position error is a univariate Gaussian distribution:

$$\left(\mathbf{e} \,\middle|\, \|\mathbf{p}\|\right) \sim N\left(\mathbf{m}_e + \delta\mathbf{m}_e, \ldots\right) \tag{37}$$

where the mean of the Gaussian approximation is defined as follows:

$$\begin{bmatrix} \mathbf{m}_p \\ \mathbf{m}_e \end{bmatrix} \tag{38}$$

The deviation in the mean and variance of the conditional position error distribution may be computed using conditional distribution theory and in the case of the multi-dimensional Gaussian, the Schur complement of $\mathbf{\Sigma}_{pe}$ is used to generate the variance.

$$\delta \mathbf{m}_e = \mathbf{c}_{ep}\mathbf{c}_{pp}^{-1}\left(\|\mathbf{p}\| - \mathbf{m}_p\right) \quad (39)$$

$$\bar{\mathbf{\Sigma}} = \mathbf{c}_{ee} - \mathbf{c}_{ep}\mathbf{c}_{pp}^{-1}\mathbf{c}_{pe} \quad (40)$$

Figure 9 shows the integration region. A lower bound is chosen to reduce the range of values for which the integration is performed and thus improve accuracy at a cost of the size of eps. At each integration point an error function must be computed. This is achieved using a highly accurate analytic approximation (Johnson & Kotz, 1995) with parameters derived in equations 39 and 40.

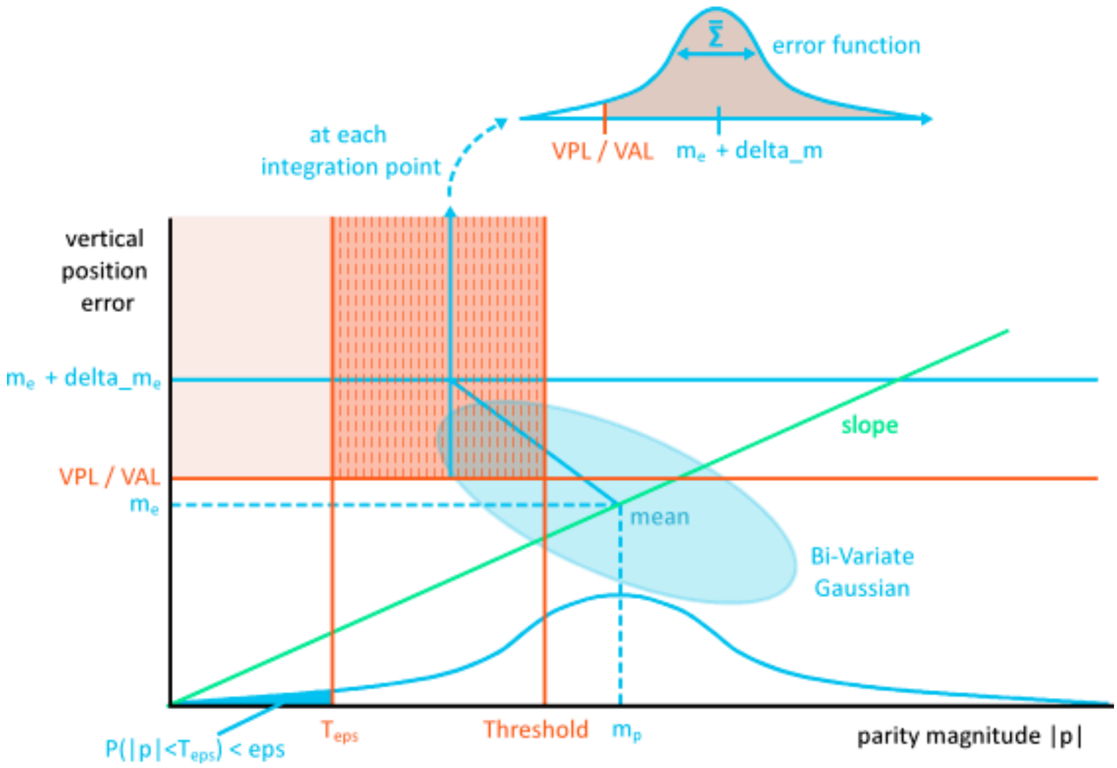

Figure 9: Weighted RAIM Integration

The numerical errors present are due to the Gaussian approximation to the chi-square distribution of parity vector, the analytic approximation to the error function and the numerical integration errors, both due to truncation and round-off error. Each of these errors has been fully analysed and their impact included in the determination of integrity risk. In order to compare to the conventional conservative bound, the integrity risk is used to search iteratively for a VPL which marginally meets the requirements.

VPL Results

The first testing phase of the new integrity computation is to compare the proposed numerical integration VPLs to those of the conventional method but also an ideal VPL derived from iteration of Monte Carlo simulation data. This was undertaken at selected airports around the globe. Figure 10 shows the VPL over an entire geometry day at Chennai international. The close match between all three procedures provides validation of the computation strategy. Expectedly the new procedure (green) is more conservative than the ideal solution (red), yet notably provides lower VPLs than the conventional method. The tracks for Sydney, JFK and Gatwick all showed similar behaviour.

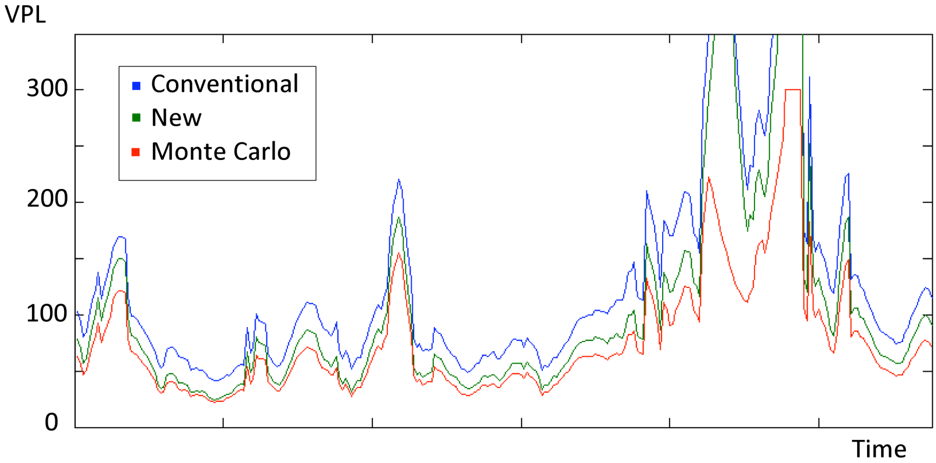

Figure 10 Chennai International Airport VPLs

Following this initial validation and testing of the proposed VPL numerical method, an availability assessment was undertaken for APVI operations (50m VAL) over a narrow strip of the world surface (1°W to 1°E) from pole to pole. This choice was made as performance varies more notably as a function of latitude than of longitude. An extensive simulation run of the entire service volume is to be completed and published in the near future.

The results of the 2 degrees of longitude assessment are shown in Figure 11. This clearly shows the marked improvement through use of the numerical procedure. The difference in availability is between 20-60%. The greatest improvement is felt at low latitude values around the equatorial regions. The performance gains may be expected to come at a considerable computational cost but performance on a standard desktop PC is such that the VPL is computed in approximately 1 second.

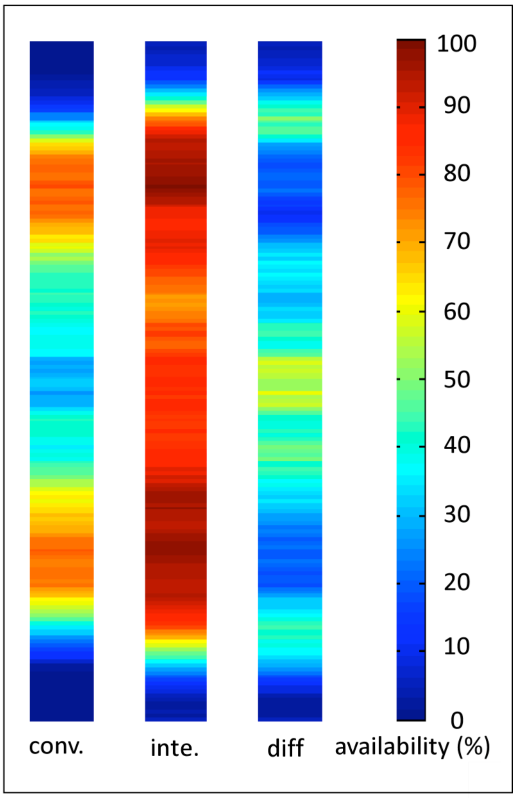

Figure 11: APVI Availability

Conclusions and Focus of Future Work

The FMEA research process undertaken has proposed a new concept of GPS failure and lead to a more accurate assessment of RAIM performance.

The proposed failure model provides greater detail and realism by defining a probability model of failure with respect to the magnitude of error bias. This is achieved for each failure mode type and allows any failure which fits one of these models to be included within the analysis. The obvious downside to such an approach is the lack of information regarding some GPS failure modes, particularly the lack of predicted probability values. However, it is hoped that our knowledge of such failures, particularly ionospheric scintillations and meteor impacts will grow significantly over the coming years. Furthermore, the advent of a civilian GNSS in the form of Galileo should ensure greater freedom of information with regard to system failures. On the downside, the continuous development of GPS satellite vehicles introduces the possibility of new failure modes not previously encountered, but given that a failure model is necessary it makes practical sense to consider a more sophisticated model than that currently employed.

The performance of the new method for computing missed alert probabilities and then VPLs has been shown to exceed that of the conventional VPL calculation. The method requires further testing and validation as well as an extension to incorporate the probability model proposed in the first half of this paper.

Acknowledgements

The authors would like to thank the UK CAA for their role in funding the Imperial College London FMEA project which includes the GPS performance monitoring for UK civilian aviation. It should be noted that the views expressed in this paper represent those of the authors only and not of the UK CAA.

References

Angus, J. E. (2007) RAIM with Multiple Faults. Navigation, Journal of the Institute of Navigation. Vol. 52, No. 4.

Bhatti, U and Ochieng, W.Y., (2007) Integrity of Integrated GPS/INS system in the presence of slowly growing errors. Part 1: A critical review. GPS Solutions Vol. 11, No. 3, July, 2007.

Brown and Chin GPS (1997) “Calculation of GPS Threshold and Protection Radius Using Chi Square Methods - A Geometric Approach” ION Red Books

Global Positioning System Standard Positioning Service Performance Standard (2001) U.S Department of Defence.

Global Positioning System Standard Positioning Service Performance Standard (2008) U.S Department of Defence.

Hwang and Brown (2005) “RAIM FDE Revisited: A New Breakthrough In Availability Performance With NIORAIM (Novel Integrity Optimized RAIM)” ION NTM 2005 San Diego CA.

Johnson and Kotz (1995) “Continuous Univariate Distributions” 2nd Edition Wiley InterScience

Lee, Y., Van Dyke, K., DeCleene, B., Studenny, J. Beckmann, M. (1996) Summary of RTCA SC-159 GPS Integrity Working Group Activities. Navigation Vol. 43, No. 3, pp307-338.

RTCA DO-229D (2006) Minimum Operational Performance Standards for GPS/WAAS Airborne Equipment

RTCA (1998) Aberration Characterization Sheet 034-01/SC159-867

Sturza, M (1988) “Navigation System Integrity Monitoring Using Redundant Measurements”

UK CAA Monitoring Documentation (2007)

Van Dyke, K., Kovach, K., Lavrakas, J., Carroll, B., (2004) Status Update on GPS Integrity Failure Modes and Effects Analysis. ION NTM, San Diego, January 2004.

Walter, T and Enge, P., (1995) “Weighted RAIM for Precision Approach” ION NTM 1995